Proceedings of the 12th International Conference on
Aluminium Alloys, September 5-9, 2010, Yokohama, Japan

pp. 308-313

Interactions between Precipitation and Annealing Phenomena during Non-isothermal Processing of an AA6xxx Alloy

Panthea Sepehrband[1], Xiang Wang[2], Haiou Jin[3], Shahrzad Esmaeili[1]

[1] Department of Mechanical and Mechatronics Engineering, University of Waterloo, 200 University Ave. West, Waterloo, ON, Canada N2L 3G1

[2] Department of Materials Science and Engineering, McMaster University, 1280 Main St. West, Hamilton, ON, Canada L8S 4L7

[3] Novelis Global Technology Centre, PO Box 8400, Kingston, ON, Canada K7L 5L9

Interactions between precipitation and annealing phenomena are investigated in a naturally aged and cold rolled AA6451 aluminum alloy during a non-isothermal annealing process which leads to significant grain refinement. It is shown that fine precipitates interact with dislocations during the initial stages of annealing and inhibit their re-arrangement and recovery. Subsequently, recrystallization is initiated by the nucleation of new grains in the well-preserved high energy sites which are uniformly-distributed within the entire structure. Precipitates interfere with the growth of the recrystallized nuclei, as well, by effective pinning of the new grain boundaries during the intermediate stages of the annealing process. Further increase in the annealing temperature results in mutually enhanced precipitate coarsening and grain boundary mobility, allowing the recrystallized grains to grow into the deformed microstructure. A fully-recrystallized fine-grained microstructure is achieved at the final stage of annealing.

Keywords: *AA6xxx Al alloys, Precipitation, Annealing, Dislocations, Grain boundary pinning*

1. Introduction

The ever increasing demands for production of light vehicles have been the motivation for many investigations on the processing, characterization and properties of aluminum alloys. Among different types of aluminum alloys, heat treatable AA6xxx alloys have attracted particular attention for replacing steels in automotive panel applications [1-3]. Although these alloys have been used for external panels in some cars, their widespread use has not been materialized partly due to their limited room temperature formability compared to steels [3, 4]. It has been considered that warm forming of aluminum panels may provide a viable solution to the formability limitation [4]. However, currently-available AA6xxx aluminum sheets do not provide desirable microstructure and mechanical behaviour at high temperatures [5-7]. Recently, a novel cost-efficient thermomechanical processing method (designated as TMPM, hereafter) has been developed, which can be implemented to achieve fine-grained AA6xxx aluminum sheets with extended ductility at warm forming temperatures [5, 8]. The TMPM involves complex interactions between precipitation and annealing phenomena. In designing the TMPM, Esmaeili and co-workers [5, 8] have postulated that formation of a fine distribution of precipitates during the early stage of annealing would obstruct rapid dislocation recovery and therefore preserve the high stored energy achieved during the deformation process. The continuation of annealing at higher temperatures would then induce uniform recrystallization either through a continuous recovery-recrystallization process or through the nucleation of new recrystallized grains at well-preserved high energy sites (i.e. discontinuous recrystallization) [5, 8]. The fine distribution of precipitates would also restrict grain growth by effective pinning of the new grain boundaries [5, 8]. The aim of this work is to examine the microstructural transformations that occur in AA6451 alloy when subjected to various stages of TMPM and provide an insight into the micro-mechanisms that lead to such grain refinement. The research is also a part of a comprehensive investigation, using both experimental and computational approaches, to evaluate the effect of the processing history on the microstructural evolution during annealing of AA6xxx alloys (e.g. [9]).

2. Experimental Methodology

The material of study is AA6451 alloy which contains (in wt pct) 0.64Mg, 0.77Si, 0.31Cu, 0.26Fe, 0.23Mn, 0.001Cr, 0.024Ti and balance Al. Samples of the alloy are thermally or thermomechanically processed to achieve the microstructural states associated with the early, intermediate and final stages of TMPM. Microstructural investigation is conducted by employing transmission electron microscopy (TEM), differential scanning calorimetry (DSC), and electron backscattered diffraction (EBSD) techniques. Microhardness measurements are performed to evaluate hardening and softening phenomena during thermal and thermomechanical processing. The processing stages for preparing TEM, DSC and EBSD test samples are schematically presented in Fig. 1. The sample identification is reported in Table 1.

TEM experiments are conducted using a Philips CM12 microscope operated at 120kV. A conventional TEM sample preparation procedure is used for preparing thin foils. DSC tests are carried out in a SETARAM C80 calorimeter in an air atmosphere and using the same heating rate as the non-isothermal annealing, i.e. 0.4˚C/min (up to 300˚C). For each test, multiple sample pieces, 10 mm × 5 mm × 1 mm in size (total mass ~ 845 mg), are placed in the test vessel while the reference vessel is kept empty. The baseline trace is acquired by running a similar test on pure Al sample (same mass as the alloy sample). The corrected final DSC trace is obtained by subtracting the baseline trace from the trace acquired for the alloy sample. DSC tests are repeated at least three times to confirm repeatability of the results. Microhardness measurements are conducted using a Leco hardness tester and applying 200g load for 20 seconds. For these tests, multiple naturally aged (*NA*) and naturally aged and cold rolled (*NA-CR*) samples are heated to various annealing temperatures in the range of 50˚C to 380˚C, with the same heating rate as the DSC test and with 25˚C intervals. Each reported hardness value is the average of seven readings. The EBSD test is conducted using a Phillips XL30S field emission gun (FEG) scanning electron microscope (SEM), equipped with a Nordlys II detector. The test is run on a region about 1.5mm x 1mm of the sample which has undergone full TMPM route (*NA-CR-380*) followed by an electropolishing procedure. HKL Channel 5 software is used for grain structure reconstruction, considering 7.5° as the threshold angle [5].

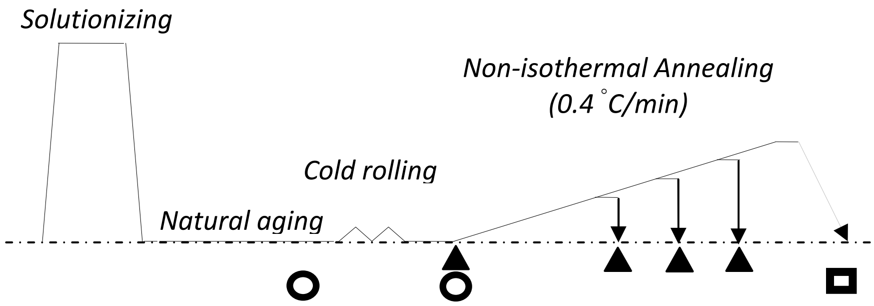

Fig. 1. Schematic presentation of the processing routes used for preparing the DSC (○), TEM (▲) and EBSD (□) samples.

Table 1. Test sample identification

Designation	Process Route	Test
NA	15 min at 560˚C + water quenching + 1 week at room temperature	DSC
NA-CR	*NA* + Cold Rolling (80% reduction in thickness)	DSC, TEM
NA-CR-180	*NA-CR* + heating from 50˚C to 180˚C (0.4˚C/min) + 20 min at 180˚C + water quenching	TEM
NA-CR-235	*NA-CR* + heating from 50˚C to 235˚C (0.4˚C/min) + 20 min at 235˚C + water quenching	TEM
NA-CR-340	*NA-CR* + heating from 50˚C to 340˚C (0.4˚C/min) + 20 min at 340˚C + water quenching	TEM
NA-CR-380	*NA-CR* + heating from 50˚C to 380˚C (0.4˚C/min) + 20 min at 380˚C + furnace cooling	EBSD

3. Results and Discussions

The result of the EBSD test on the *NA-CR-380* sample provides information on the grain structure that is obtained by implementing TMPM on AA6451 alloy. As Fig. 2 demonstrates, a fully-recrystallized microstructure with a relatively uniform and narrow grain size distribution is achieved. The average grain size of the sheet is 11.4 μm, while a large fraction of the grains have an average diameter below 10 μm. The micro-mechanisms that lead to such grain refinement are analysed below using the results of TEM, DSC and microhardness tests.

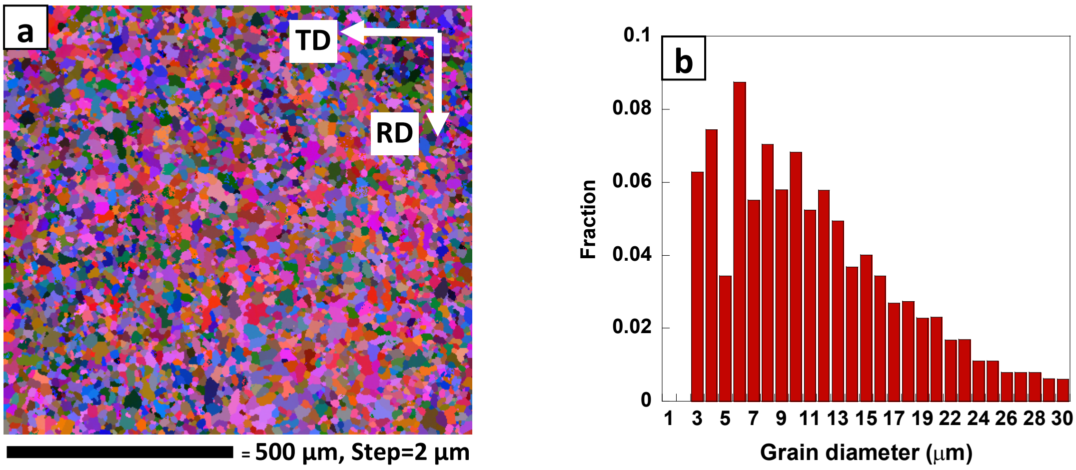

Fig. 2. (a) EBSD map showing recrystallized grain structure of *NA-CR-380* in the rolling plane, (b) Average grain diameter distribution for the EBSD map.

The effect of precipitates on dislocation re-arrangement is first examined by analyzing the results of the TEM tests on the as-deformed structure of the *NA-CR* sample and the annealed *NA-CR-180* and *NA-CR-235* samples. Generally, metals with high stacking fault energies, such as aluminum, have high tendency for dynamic recovery during deformation and, hence, formation of dislocation cell structures [10]. However, the TEM study on the as-deformed *NA-CR* sample reveals a uniform distribution of dislocations, as shown in Fig. 3a, indicating that dynamic recovery during deformation has been inhibited. This effect can be related to the presence of natural aging clusters [11] interacting with dislocations and/or the solute drag effect [12]. The dislocation distributions in the *NA-CR-180* and *NA-CR-235* samples, as shown in Fig. 3b and 3c, respectively, do not represent cell structure formation, either, and a high density of uniformly-distributed dislocations is present in each case. Dark field TEM studies at higher magnification reveal the evidence for the presence of very fine precipitates in the *NA-CR-180* sample, Fig. 3d, and a fine and uniform distribution of well-grown precipitates in *NA-CR-235* sample, Fig. 3e. A selected area diffraction pattern (SADP) of *NA-CR-235* sample is presented in Fig. 3f. The position of streaks in the SADP [13] provides evidence for the coexistence of two types of precipitates at this annealing condition. These precipitates interfere with dislocation movement and thus the recovery process. Mutually, dislocation cores provide easy paths for solute diffusion, which in turn lead to rapid precipitate growth and coarsening.

Further TEM analysis of the *NA-CR-235* sample provides evidence for the formation of new recrystallized nuclei, as shown in Fig. 4a. The nuclei are observed in several regions of the microstructure with no prominent favoured nucleation site in the deformed grain. Such observation is linked to the presence of high levels of stored energy inside the grains due to the prevention or delay of the recovery process. As the arrows in Fig. 4a demonstrate, grain boundaries of the newly formed nuclei are pinned by fine precipitates and therefore no major growth is observed at this intermediate annealing stage. However, further annealing to higher temperatures results in coarsening of precipitates and thus reduces the precipitate pinning effect. Such effect, in turn, allows recrystallized nuclei to grow and a substantially-recrystallized structure to form after annealing of the *NA-CR* sample to 340°C. A TEM micrograph of *NA-CR-340* sample, which shows two recrystallized grains adjacent to a remaining deformed area, is shown in Fig. 4b. It is evident that precipitates within the recrystallized grains are larger than the precipitates within the deformed region. Considering high diffusion rates along grain boundaries, these large precipitates are mainly the preferentially coarsened precipitates that were initially located on the pinned boundaries. The above observations on the nucleation of new grains and co-existence of adjacent recrystallized and deformed grains may suggest that recrystallization occurs mainly in a discontinuous manner. More work is underway to clarify the recrystallization behaviour.

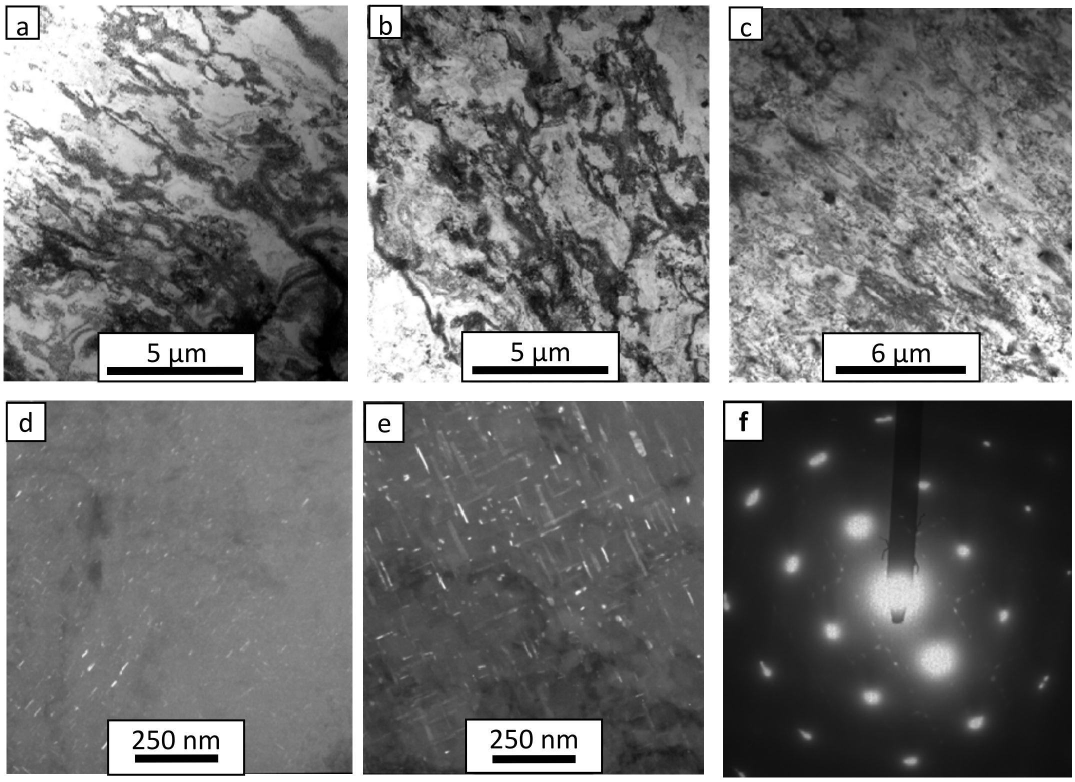

Fig. 3. Bright field (a-c) and dark field (d, e) TEM micrographs in $[001]_{Al}$ projection of (a) *NA-CR*, (b, d) *NA-CR-180* and (c, e) *NA-CR-235* samples; (f) A SADP obtained from *NA-CR-235* at $[001]_{Al}$ zone axis.

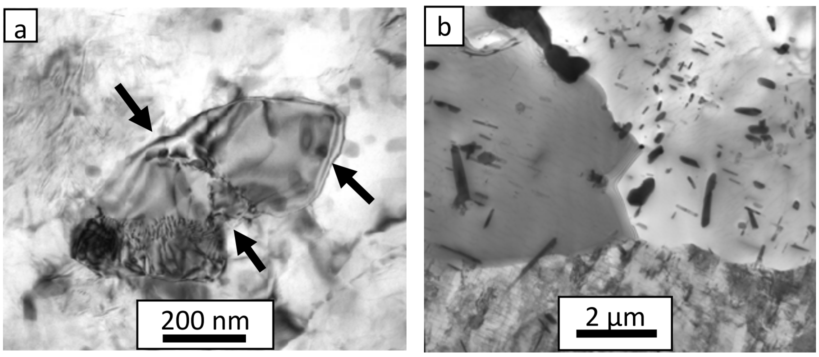

Fig. 4. Bright field TEM micrographs in $[001]_{Al}$ projection of (a) *NA-CR-235*, and (b) *NA-CR-340* samples.

The interactions between precipitation and the recovery-recrystallization processes are further examined by analyzing the results of the combined DSC and microhardness tests on *NA* and *NA-CR* samples (Fig. 5). The results of the tests on the *NA* sample provide information on the precipitation hardening behaviour in the absence of prior deformation. The DSC trace for this sample reveals three exothermic peaks in the temperature range of 50-300°C. These peaks represent the sequential formation of early stage precipitates (Peak *A*), with small hardening effect, and the well-developed precipitates (peaks *B* and *C*), which are highly effective in increasing hardness. The maximum level of hardness coincides with the completion of precipitation event *B*. The subsequent decrease in hardness is therefore attributed to the coarsening of *B*-type precipitates and their replacement by *C*-type precipitate phase. The above knowledge on the *NA* sample, as well as the TEM results, help to analyse the results of the tests on *NA-CR* sample which present overlapping effects of precipitation and recovery-recrystallization processes. The DSC trace of the *NA-CR* sample exhibits only two exothermic peaks, i.e. peak *I* centered at 130˚C, and peak *II* centered at 180˚C. The TEM observations of precipitates and the lack of appreciable recovery and recrystallization in *NA-CR-180* and *NA-CR-235* samples, as well as the well-established reports on the small heat effects due to recovery/recrystallization processes [10, 14], suggest that the two peaks are associated with precipitation events only. Furthermore, peak *I* is associated with the formation of early-stage precipitates, as in the case of *NA* sample, while peak *II* represents the formation of more advanced precipitate forms, similar to the precipitates formed in the microstructure of *NA-CR-180* and *NA-CR-235* samples. These precipitates are prone to enhanced coarsening due to the presence of a high density of uniformly-distributed dislocations, as observed in *NA-CR-180* sample. In addition, the presence of two types of precipitates in the microstructure of *NA-CR-235* sample suggests that peak *II* is an overlap of two precipitation events. Although the precipitation event during non-isothermal annealing of *NA-CR* sample to 150˚C results in a slight increase in the hardness, continuation of annealing to higher temperatures leads to hardness reduction. Comparing the hardness results in *NA-CR* and *NA*, it is noticed that the two samples show similar trends in the decrease of hardness with increasing temperature at temperatures below 300˚C, indicating the major role of precipitate coarsening in the softening of both samples during the corresponding heat treatment processes. Interestingly, however, the two samples demonstrate significantly different softening behaviour when the temperature is increased beyond approximately 300˚C: while the hardness of the *NA* sample gradually decreases, that of *NA-CR* sample shows a sudden fall. It is well known that temperature rise results in increasing grain boundary mobility [10]. In addition, the kinetics of precipitate coarsening is enhanced with the increase in temperature [15]. In the present case, it is speculated that such combined effects result in accelerated recrystallization in the temperature range between 300˚C and 340˚C. The continuation of annealing beyond 340˚C results in a hardness plateau which corresponds to the completion of recrystallization processes, as also evidenced by the TEM and EBSD results on *NA-CR-340* and *NA-CR-380* samples, respectively.

4. Conclusions

Interactions between precipitates and annealing phenomena in an AA6451 aluminum alloy during a grain refining thermomechanical process have been investigated. It has been found that uniformly distributed fine precipitates interact with the recovery process at the early stages of annealing. As a result, recrystallization appears to initiate by the nucleation of new grains in the well-preserved high energy sites which are uniformly-distributed within the entire structure. The newly formed grain boundaries are effectively pinned by fine precipitates. The mutual effects of precipitate coarsening and enhanced grain boundary mobility at the late stages of annealing result in the completion of the recrystallization process and the formation of a fine-grained microstructure.

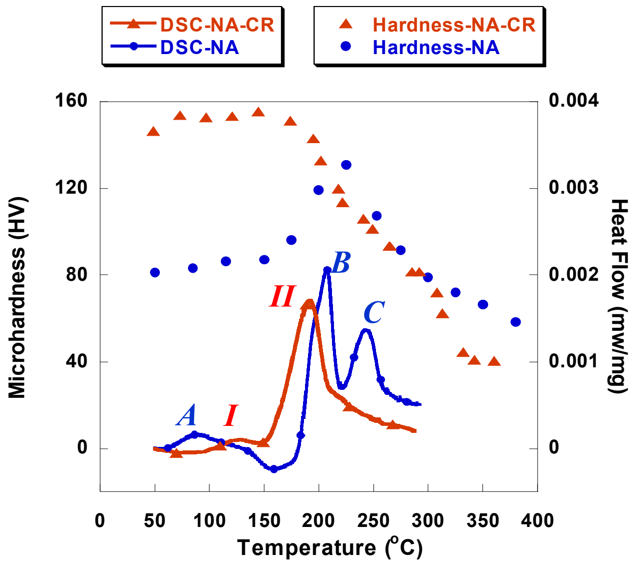

Fig. 5. DSC thermograms and hardness evolution of naturally aged and cold rolled (*NA-CR*), and naturally aged (*NA*) samples.

5. Acknowledgement

This work was supported by joint grants from Natural Sciences and Engineering Research Council of Canada (Collaborative Research and Development Program), Novelis Corporation, and Ontario Research Fund (Research Excellence Program through the Initiative for Automotive Manufacturing Innovation, IAMI). The very helpful discussions with Dr. D.J. Lloyd and Dr. B. Poorganji are gratefully acknowledged.

References

[1] G.B. Burger, A.K. Gupta, P.W. Jeffrey, and D.J. Lloyd, Mater. Char. 35 (1995) 23-39.
[2] D.J. Lloyd, in: D.S. Wilkinson, W.J. Poole (Eds.), Advances in Industrial Materials, The Metallurgical Society of CIM, Montreal, 1998, 3-17.
[3] J. Hirsch: Materials Forum. 28 (2004) 15-23.
[4] D. Daniel, G. Guiglionda, P. Litalien and R. Shahani: Mater. Sci. Forum. 519-521 (2006) 795-802.
[5] S. Esmaeili, D. Lloyd and H. Jin: Submitted for publication.
[6] R.N. Carrick: MASc Thesis, University of Waterloo, Canada, 2009.
[7] W.J. Kim and S.J. Yoo: Scripta Mater. 61 (2009) 125-28.
[8] S. Esmaeili, D. Lloyd and H. Jin: PCT application filed by the University of Waterloo, 2009.
[9] P. Sepehrband and S. Esmaeili: Scripta Mater. In Press.
[10] F.J. Humphreys and M. Hatherly: *Recrystallization and Related Annealing Phenomena*, 2 ed. (Pergamon Press, Oxford, 2004) 13, 173-174.
[11] S. Esmaeili and D.J. Lloyd: Scripta Mater. 50 (2004) 155-158.
[12] E. Nes: Acta Metall. Mater. 43 (1995) 2189-2207.
[13] W.F. Miao and D.E. Laughlin: Metall. Mater. Trans. 31A (2000) 361-371.
[14] N. Gao, M.J. Starink and T.G. Langdon: Mater. Sci. Tech. 23 (2009) 687-698.
[15] D.A. Porter and K.E. Easterling: *Phase Transformations in Metals and Alloys*, 2 ed. (Chapman and Hall, London, 1992) 314.